Electron and positron scattering cross sections for propene and cyclopropane

C. Makochekanwa,[1,2,*] M. Hoshino,[1] H. Kato,[1] O. Sueoka,[2] M. Kimura,[3] and H. Tanaka[1]
[1]*Department of Physics, Sophia University, Tokyo 102-8554, Japan*
[2]*Faculty of Engineering, Yamaguchi University, Yamaguchi 755-8611 Japan*
[3]*Graduate School of Sciences, Kyushu University, Fukuoka 812-8581, Japan*
(Received 7 February 2008; published 22 April 2008)

In this paper we investigate electron and positron total and electron vibrational excitation scattering cross sections for propene and cyclopropane molecules. The electron and positron total cross sections were measured over the energy range 0.2–1000 eV using a retarding-potential time-of-flight method while the electron impact vibrational excitation cross sections were measured using a crossed-beam method. For both molecules, bending and stretching vibrational modes are studied at loss energies 0.12 and 0.37 eV, respectively, for propene, and 0.13 and 0.37 eV, respectively, for cyclopropane, at the scattering angle of 90° and impact energy range 1–16 eV.

DOI: 10.1103/PhysRevA.77.042717 PACS number(s): 34.80.Bm, 34.80.Dp, 36.10.Dr

I. INTRODUCTION

Recently the so-called electron-driven processes in molecular collisions have invited a great deal of research interest due to their various applications as well as the physics involved in the scattering dynamics. In particular, it has been established that hydrocarbons are produced in fusion plasmas, as by-products of plasma irradiation at the diverter regions and, to some extent, at the tokamak walls following repeated sputtering of the graphite walls (see, for example, Ref. [1]). Furthermore, lighter linear hydrocarbons are also of interest as they play important roles in chemical vapor deposition (CVD) reactions [2]. It is needless to point out that in any of these processes, mentioned just as a few examples, secondary collision processes between these molecules and the free electrons, inevitably available in the plasma, lead to a whole variety of important processes. This means that, in order to accurately model and control these plasma processes, all the relevant electron collision processes' cross sections need to be accurately known. In particular, cyclopropane (hereafter referred to as c-C_3H_6) has been reported to constitute a significant proportion of the gaseous part of cold-edge fusion plasmas [3].

The recent developments of trap-based positron beams have gone a long way in enabling the study of positron-atom and-molecule collision processes with improved resolution and intensities. As summarized recently by Surko *et al.* [4], state-resolved measurements of electronic and vibrational excitation cross sections and annihilation rate measurements have been achieved for some simple molecules. At energies below that for the formation of the positronium (Ps) atom (a bound state of an electron and positron), chemical reactions may be induced by low-lying transient anion and cation states formed by the attachment of electrons and positrons, respectively. These quasibound states are due to the short-range polarization interaction induced when an electron or positron approaches a target molecule. This dissociative positron attachment (DPA) is only just beginning to be studied, but the first results indicate that hydrocarbons can effectively bind positrons while fluorocarbons do not. Thus, positron scattering is no longer just a tool for better understanding of electron impact phenomena only, but is now offering some interesting collision study areas.

A variety of studies have been carried out on c-C_3H_6 owing mainly to its ring molecular structure, as well as in combination with its isomer partner, i.e., the linear C_3H_6 molecule. Literature data on electron and positron scattering focusing on C_3H_6 alone have remained scarce and fragmentary to date. Studies available in the literature on both C_3H_6 and c-C_3H_6 include the experimental 5–400 eV electron and positron total cross sections (TCSs) by Floeder *et al.* [5], 4–500 eV electron TCSs by Nishimura and Tawara [6], and 0.5–370 eV electron TCSs by Szmytkowski and Kwitnewski [7]. Experimental and theoretical ionization cross sections (ICSs) on both molecules are available from Nishimura and Tawara [8] and Deutsch *et al.* [9], respectively. Electron impact elastic differential cross sections (DCSs) for both molecules have been studied mainly theoretically [10–13]. To our knowledge there exists only one measurement on electron impact elastic and vibrational excitation of c-C_3H_6 [14], besides our recently published electron impact elastic DCS data on both molecules [13].

Literature studies focusing on c-C_3H_6 alone include the theoretical work of Jiang *et al.* [15] on 10–1000 eV electron impact TCSs, the high-resolution electron impact vibrational excitation studies by Allan [16], and the quantum mechanical calculations carried out to investigate a number of the vibrational modes of these molecules by Curik and Gianturco [17]. High-resolution electron energy loss spectroscopy has also been employed to study singlet-triplet excitation, and inner-shell and valence-shell electronic excitation of this molecule [18–20], while photoabsorption and photoelectron spectra were also studied and helped in establishing its electronic states [21,22]. The few studies solely focusing on C_3H_6 include low-energy electronic excitation spectra measurements using the trapped-electron technique [23], electron swarm experiments for momentum transfer and vibrational

*Present address: Atomic and Molecular Physics Laboratories, RSPhySE, Australian National University, Canberra, ACT 0200, Australia.

excitation [24], and measurements on energy loss spectra [25].

In this work we carry out a comparative experimental investigation of electron and positron TCSs over the range 0.2–1000 eV. Discussions of the resonance features observed in the electron TCSs are greatly aided by a combined study with vibrational excitation cross sections. This work is also necessitated by the discrepancies that currently exist between the existing four sets of electron TCSs, and that only one TCS data set exists for positron TCSs over the limited energy range of 4–400 eV [5].

II. PROCEDURES

A. Total cross section experiments

For these measurements a retarding-potential time-of-flight (RP-TOF) method was used. The apparatus for this has been reported in detail elsewhere [26] and thus is only briefly summarized here. The source for the electron and positron beams is a ^{22}Na radioisotope with an activity of ~80 μCi. The energy resolution, determined by the RP-TOF apparatus, is an average 0.3 eV below 4 eV. However, the energy resolution is dependent on the impact energy and increases with increase in impact energy (see Ref. [27]). The TCS values were derived from the Beer-Lambert attenuation equation

$$Q_t = -\frac{1}{n\ell}\ln\frac{I_g}{I_v}, \tag{1}$$

where I_g and I_v refer to the projectile beam intensities transmitted through the collision cell with and without the target gas of number density n, respectively. ℓ refers to the effective length of the collision cell and was established by normalizing our measured positron-N_2 TCS to the positron-N_2 TCS data of Hoffman *et al.* [28]. The energy calibration was done using positron-N_2 TOF spectra measured at 20 energies chosen in the range 8–150 eV [29]. The TCS results presented in this paper were confirmed to be pressure independent in the present energy range by independent electron impact test experiments. Some of the results for *c*-C_3H_6 are shown in Fig. 1.

This TCS apparatus setup has specifically been designed to have a collision cell with wide entrance and exit apertures (i.e., 3 mm in radius) for the weak positron beam intensities. However, this, and the use of a magnetic field for beam transportation (4.5 G for electrons and 9 G for positrons), brings with it the problem of forward-scattered electrons and positrons being detected by the Ceratron detector—which is undesirable, and thus needs to be corrected for. The procedure for this entails the use of DCS data for the molecule under study. The detailed correction procedure has been described previously [30,31]. The DCSs used for the correction of the electron data presented in this paper are from our previous study [13], for both molecules. The correction rates, for example, amounted to about 3.7% at 0.8 eV, 2.6% at 10 eV, and 4% at 60 eV and decreases continually toward higher energies, i.e., 2.6% at 600 eV, for *c*-C_3H_6. For C_3H_6 these rates were 3%, 2.4%, 3.3%, and 1.3% at 0.4, 10, 60, and 600 eV, respectively. For positron TCSs, however, this correction could not be done because of lack of DCS data, and thus the TCSs are presented as measured for both molecules.

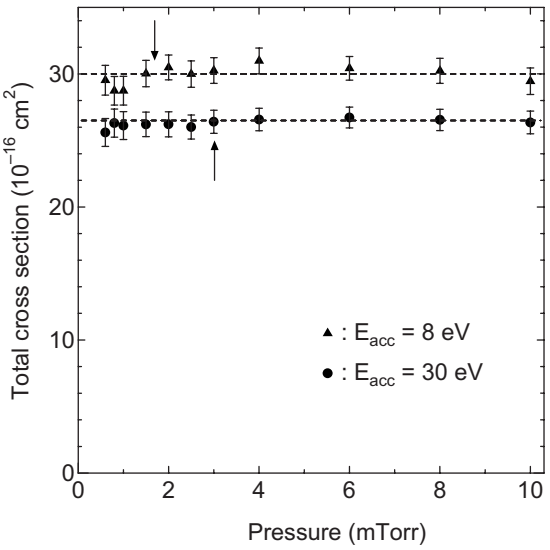

FIG. 1. Electron TCSs for *c*-C_3H_6 plotted against gas pressure for the two impact energies 8 and 30 eV. The beam intensity attenuations (I_g/I_v) of 1/3 used for the TCS measurements are shown by the arrows. Error bars show the total uncertainties derived as explained in the text.

The errors shown in the data in Tables I and II are the sum total uncertainties; made up of contributions from statistical and gas pressure fluctuations and the effective collision cell length calibration. These total uncertainties were estimated to be 2.8%–4.0% and 5.2%–20% for electron and positron impact, respectively, for C_3H_6, and 5.4%–6.4% and 6.2%–11.3% for electron and positron impact, respectively, for *c*-C_3H_6.

B. Vibrational excitation experiments

These experiments were carried out using a crossed-beam apparatus, which has already been extensively described in previous publications [32] and is only briefly summarized here. Electrons from a 180° monochromator intercept an effusive molecular beam at right angles and the scattered electrons are energy analyzed in a second 180° hemispherical system. To keep the transmission of the electrons constant in the lens system, programmable power supplies are used to ramp the mid-element potentials of the monochromator exit and analyzer entrance lenses as required. Both the monochromator and the analyzer are enclosed in differentially pumped boxes, to reduce the effect of the background gases and to minimize the stray electron background. The target molecular beam is produced by effusing the gas through a nozzle with an internal diameter of 0.3 mm and a length of 5 mm. The spectrometer and the nozzle are heated to a temperature of about 70 °C to reduce the possibility of contamination during measurements. The overall energy resolution of the present measurements was about 35–40 meV, and the angular resolution was $\pm 1.5°$.

The vibrational DCSs were measured while sweeping the impact energy from 1 to 16 eV, at loss energies 0.12 and 0.37

TABLE I. Cyclopropane (c-C_3H_6) electron and positron TCSs (10^{-16} cm^2). Errors indicate total uncertainties derived as explained in the text.

Energy (eV)	Electron	Positron	Energy (eV)	Electron	Positron
0.7		11.6 ± 0.7	11	31.9 ± 1.0	19.3 ± 0.9
0.8	17.5 ± 0.8		12	31.8 ± 1.0	17.2 ± 0.8
1.0	17.2 ± 0.5	13.0 ± 0.7	13	31.6 ± 1.0	16.5 ± 0.7
1.2	17.6 ± 0.5		14	31.2 ± 1.0	17.5 ± 0.8
1.3		15.3 ± 0.8	15	31.0 ± 1.0	19.0 ± 1.0
1.4	17.7 ± 0.5		16	30.4 ± 0.9	18.8 ± 1.1
1.6	17.6 ± 0.5	17.6 ± 0.9	17	30.4 ± 0.9	18.6 ± 0.9
1.8	17.3 ± 0.6		18	29.7 ± 0.9	19.2 ± 1.0
1.9		18.0 ± 0.9	19	29.8 ± 0.9	19.2 ± 1.0
2.0	17.2 ± 0.6		20	29.7 ± 0.9	20.3 ± 1.1
2.2	17.3 ± 0.6	17.1 ± 0.8	22	29.4 ± 0.8	19.7 ± 0.9
2.5	18.0 ± 0.6	17.3 ± 0.9	25	28.5 ± 0.9	19.1 ± 1.0
2.8	17.9 ± 0.6	17.2 ± 0.8	30	27.5 ± 0.9	19.9 ± 1.1
3.1	18.2 ± 0.6	17.3 ± 0.8	35	25.8 ± 0.9	
3.4	18.2 ± 0.6	17.3 ± 0.8	40	25.4 ± 0.8	19.4 ± 0.7
3.7	19.1 ± 0.7	18.0 ± 0.8	50	23.8 ± 0.7	18.5 ± 0.7
4.0	20.4 ± 0.7	17.3 ± 0.7	60	22.3 ± 0.8	17.7 ± 0.7
4.5	22.4 ± 0.7	18.1 ± 0.8	70	20.2 ± 0.8	16.8 ± 0.6
5.0	26.4 ± 0.8	17.8 ± 0.8	80	19.7 ± 0.7	16.7 ± 0.7
5.5	27.3 ± 0.9	19.2 ± 0.9	90	19.1 ± 0.6	15.8 ± 0.6
6.0	28.9 ± 0.9	19.2 ± 0.9	100	18.0 ± 0.6	14.6 ± 0.6
6.5	29.0 ± 1.0	19.4 ± 0.9	120	16.0 ± 0.5	14.3 ± 0.6
7.0	30.2 ± 1.0	20.0 ± 0.9	150	14.7 ± 0.5	13.4 ± 0.6
7.5	30.4 ± 1.0	19.6 ± 0.9	200	12.7 ± 0.4	11.3 ± 0.5
8.0	32.0 ± 1.1	19.2 ± 0.9	250	11.3 ± 0.4	10.2 ± 0.5
8.5	31.6 ± 1.1	19.1 ± 0.9	300	10.3 ± 0.3	8.8 ± 0.6
9.0	32.6 ± 1.1	18.9 ± 0.9	400	8.4 ± 0.3	7.1 ± 0.5
9.5	32.5 ± 1.2	19.5 ± 0.9	500	7.1 ± 0.2	7.0 ± 0.6
10	32.3 ± 1.0	19.2 ± 0.8	600	6.4 ± 0.2	6.2 ± 0.4

eV for propene, and 0.13 and 0.37 eV for cyclopropane, and the common scattering angle of 90°. Absolute cross sections were obtained by the relative flow technique [33] using helium as the reference gas. Experimental errors in the vibrational excitation DCS were of order 15%–20%.

III. RESULTS AND DISCUSSION

For each molecule, the order of presentation is that a joint electron impact TCS and vibrational excitation cross section discussion is carried out first. Since our electron TCS results have been partly presented before (see Refs. [13,34]), discussions are tilted toward probing the resonances using the vibrational excitation cross sections, and the comparative study with literature results. Positron TCSs are then analyzed, before the comparative study with the electron impact TCSs at the end. The numerical values for the electron and positron TCSs for these two molecules are presented in Tables I and II, together with the total uncertainties associated with each value.

A. Electron impact

1. c-C_3H_6

In Fig. 2 we show all the five sets of TCS results from the literature, together with the ionization cross section results of Nishimura and Tawara [8]. In general, except for the continually increasing result of Jiang *et al.* [15], all the TCS results show similarity of energy dependence. For example, the TCS results are characterized by (i) weak humps at about 1.5 and 2.6 eV, (ii) the slight change of slope at around 6 eV, (iii) the main resonance peak centered at about 9.5 eV, and (iv) the decreasing trend beyond the main peak toward the highest energy for each, albeit showing some change of slope around 60 eV.

As a way of probing the nature and origin of these peaks in electron impact TCSs, we carried out a series of experiments investigating the vibrational excitation channel. This choice was based on an understanding that, although in the elastic scattering channel elastic scattering via resonances is in general masked by the direct elastic component, reso-

TABLE II. Propene (C_3H_6) electron and positron TCSs ($\times 10^{-16}$ cm^2). Errors indicate total uncertainties derived as explained in the text.

Energy (eV)	Electron	Positron	Energy (eV)	Electron	Positron
0.2		9.4 ± 1.6	11	39.8 ± 1.1	22.4 ± 1.4
0.4	21.3 ± 0.8	8.0 ± 1.6	12	38.2 ± 1.1	22.1 ± 1.4
0.6	19.5 ± 0.7	10.1 ± 1.6	13	38.9 ± 1.1	23.5 ± 1.6
0.8	19.3 ± 0.7	15.0 ± 2.2	14	38.4 ± 1.1	22.9 ± 1.4
1.0	19.7 ± 0.7	14.7 ± 1.9	15	37.6 ± 1.1	24.3 ± 1.7
1.2	21.1 ± 0.7		16	36.8 ± 1.1	25.3 ± 1.8
1.3		14.3 ± 1.8	17	35.5 ± 1.0	25.0 ± 1.8
1.4	23.0 ± 0.8		18	34.6 ± 1.0	21.7 ± 1.8
1.6	24.8 ± 0.8	15.5 ± 2.2	19	34.4 ± 1.0	23.2 ± 1.7
1.8	27.2 ± 0.9		20	33.9 ± 1.0	22.7 ± 1.7
1.9		17.4 ± 2.3	22	33.7 ± 0.9	21.3 ± 1.1
2.0	29.1 ± 1.0		25	31.6 ± 0.9	21.8 ± 1.8
2.2	29.9 ± 1.0	14.8 ± 2.0	30	29.4 ± 0.9	18.4 ± 1.1
2.5	28.4 ± 0.9	18.2 ± 3.0	35	28.7 ± 0.9	
2.8	26.7 ± 0.9	19.0 ± 2.9	40	27.3 ± 0.9	17.1 ± 1.4
3.1	25.7 ± 0.9	19.5 ± 2.8	50	24.7 ± 0.8	16.7 ± 1.2
3.4	25.9 ± 0.9	20.0 ± 2.7	60	22.5 ± 0.7	17.6 ± 1.2
3.7	25.7 ± 0.9	20.6 ± 2.8	70	21.6 ± 0.7	
4.0	26.4 ± 0.9	21.2 ± 2.7	80	20.7 ± 0.6	15.3 ± 1.0
4.5	28.0 ± 0.9	21.9 ± 1.8	90	18.6 ± 0.6	
5.0	29.7 ± 1.0	23.0 ± 1.6	100	17.7 ± 0.5	15.4 ± 1.0
5.5	33.4 ± 1.0	22.3 ± 1.3	120	17.0 ± 0.5	14.6 ± 1.0
6.0	34.7 ± 1.1	22.3 ± 1.3	150	14.9 ± 0.5	13.5 ± 0.7
6.5	37.0 ± 1.1	23.4 ± 1.3	200	12.4 ± 0.4	11.6 ± 0.6
7.0	37.8 ± 1.1	23.2 ± 1.4	250	11.3 ± 0.4	10.9 ± 0.6
7.5	39.7 ± 1.2	23.2 ± 1.4	300	9.6 ± 0.3	9.8 ± 0.6
8.0	40.1 ± 1.2	22.7 ± 1.5	400	7.9 ± 0.3	8.1 ± 0.4
8.5	40.3 ± 1.2	22.6 ± 1.5	500	7.0 ± 0.2	7.2 ± 0.4
9.0	40.5 ± 1.2	23.7 ± 1.5	600	6.1 ± 0.2	6.5 ± 0.3
9.5	40.2 ± 1.2	24.2 ± 1.8	800	4.8 ± 0.1	5.3 ± 0.2
10	40.1 ± 1.1	21.9 ± 1.3	1000	4.1 ± 0.1	4.4 ± 0.2

nances can in most cases be clearly revealed in vibrational excitation functions for experiments done while sweeping impact energies across the resonance region. In Fig. 3(a) we show an energy loss spectrum that was measured for these molecules at an impact energy of 8 eV and scattering angle 70°. At loss energies of 0.13 and 0.37 eV we clearly observe peaks corresponding to two of the dominant modes of vibration for c-C_3H_6, i.e., bending ν_2 and C-C stretching ν_3, respectively. Figures 3(b) and 3(c) show the DCS functions for vibrational excitation of these two modes measured with the energy losses fixed at 0.13 and 0.37 eV while sweeping the electron impact energy over the range 1–16 eV.

(i) The 1.5 eV weak peak observed in the TCSs, although only observed in our report [34] and not reported in the only other previous work that covered this range, i.e., that of Szmytkowski *et al.* [7], might have origins in both the C-C ring deformation (ν_{11}) and symmetric ring stretching (ν_3) vibrational excitations, which exhibit weakly rising excitation functions below 2 eV [16]. The current vibrational excitation results (Fig. 3) do not show this feature. (ii) Our vibrational excitation results [Figs. 3(b) and 3(c)] clearly show that the shoulder at about 6 eV in the TCS can be attributed to a resonance phenomenon arising from a combination of the excitation of the bending ν_2 and stretching ν_3 modes. Earlier studies had also observed this for the stretching vibrational excitation (ν_3 mode) motion of the C-C (ring) [11,16,17,35]. The higher resolution and vibrationally finer inelastic measurements by Allan and Andric [16] reveal the further information that this resonance has origins also in the higher-ν_3 vibrational modes (i.e., $2\nu_3$ and $3\nu_3$ modes), and minor contributions from the ring deformation (ν_{11}) vibrational excitation as well. (iii) The main broad peak centered at about 9.5 eV in the TCSs is also observed in the cross sections for the stretching ν_3 vibrational mode. This peak feature at around this energy region has been systematically observed in earlier studies of both TCSs and vibrational ex-

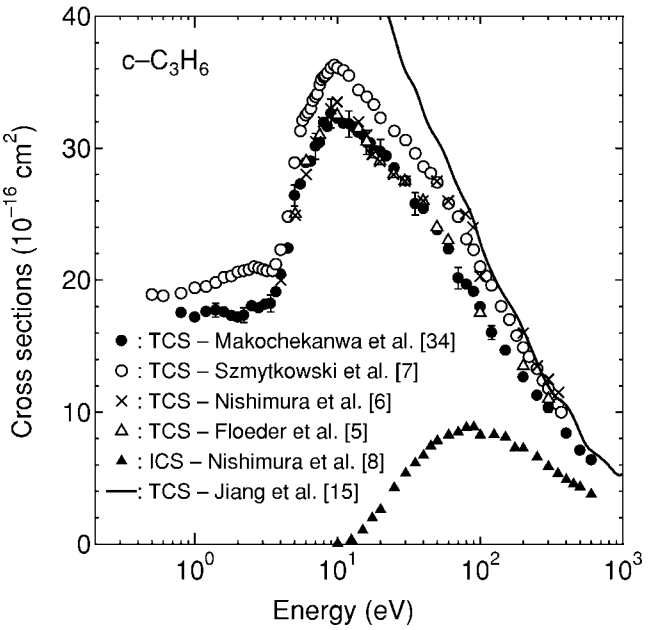

FIG. 2. c-C_3H_6 electron impact TCSs and ICSs from the literature, including the TCS result from our preliminary report [34].

citation cross sections, found to be characteristic of hydrocarbon molecules, and attributed to resonances arising from the trapping of the incident electron into the σ^* orbital [16,36]. Beyer *et al.* [11] and Curik and Gianturco [12] observed a similar peak around this energy in their elastic integral cross sections (ECSs) and assigned it to the E' symmetry. Once again we refer to the high-resolution vibrationally inelastic measurements of Allan and Andric [16] to shed more light on the nature of this broad resonance feature. These results show that several vibrational modes are contributing to this broad resonance peak; i.e., the $\nu_1 + \nu_2$ (peak at 7.6 eV), $2\nu_1$ (peak at 8.1 eV), ν_2 (CH_2 scissors, peak at 8.6 eV), and ν_{11} (C-C ring deformation, peak at 9.5 eV) modes.

Although we do not present integral vibrational excitation cross sections in this work, we carry out a rough analysis of the TCS constituents, i.e., based on the TCSs and ECSs from our preliminary study [13], the ICS results of Nishimura and Tawara [8], and the current vibrational excitation cross sections. Both the ECS (though not reproduced here) and the current vibrational excitation cross section results reproduce well the structures observed in the TCSs. The elastic channel clearly dominates scattering events below about 6 eV, as it contributes more than 90% of the TCS in this region. The difference should be mainly due to the vibrational excitation channel. Significant differences between the ECSs and the TCSs start to emerge above 7 eV, as expected from the opening up of the electronic excitation channel. The ICS channel becomes the dominant contributor to the TCS above 50 eV, i.e., constituting about 50% of the TCS at 100 eV, before overtaking the ECS in magnitude above this energy.

2. Comparison of our TCSs with other results

Since the subjects of our preliminary studies [13,34] were not studies of TCSs, even though we made use of the TCS

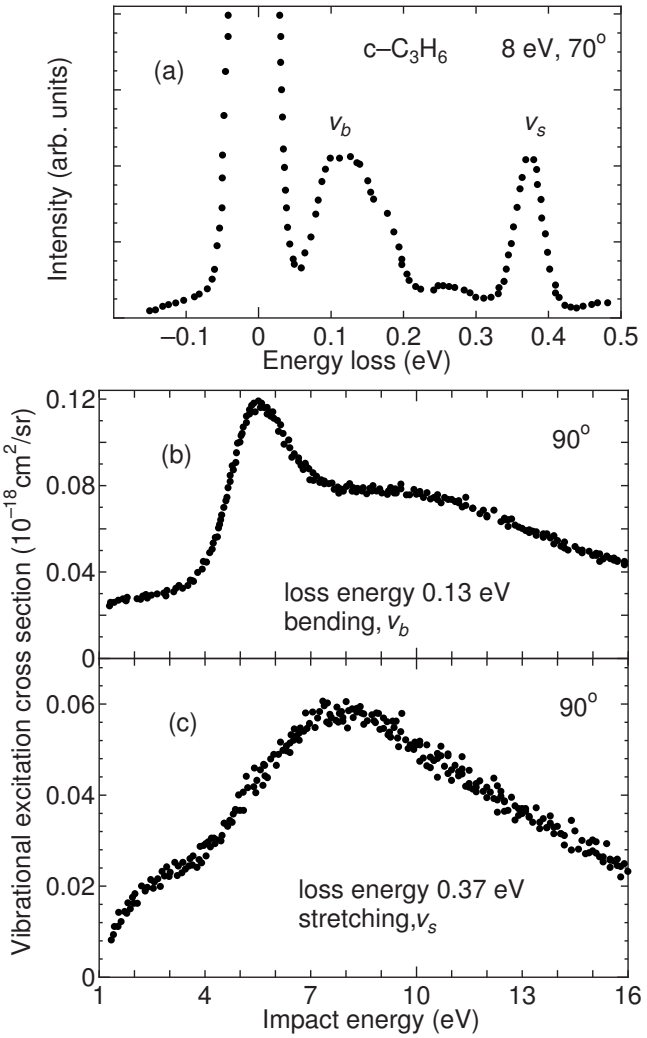

FIG. 3. c-C_3H_6 electron impact. (a) Energy loss spectrum, and vibrational excitation cross sections for the (b) bending ν_2 mode, and (c) C-C stretching ν_3 mode.

results, we carry out a short comparison of our TCSs with the literature data. Although our result agrees well both qualitatively and quantitatively with the Floeder *et al.* [5] result over all the energy range of overlap, only good qualitative agreement is observed with the other three data sets. The Szmytkowski *et al.* [7] result, however, clearly shows the 2.6 eV peak, observed in our result only as an unpronounced small shoulder. The theoretical result by Jiang *et al.* [15] shows rapidly rising TCSs below 30 eV, in contrast with the current and previous experimental publications. The Szmytkowski *et al.* result is the highest of the four experimental data sets, and is higher than our result at almost all of the energy range of overlap, with the largest difference being at the main resonance maximum, where it reaches about 12%. At energies 4–40 eV our results nearly equal the results of Floeder *et al.* [5] and Nishimura and Tawara [6]. Above 60 eV, the Nishimura and Tawara result approaches the Szmytkowski *et al.* one, while our result remains in good agreement with the Floeder *et al.* data.

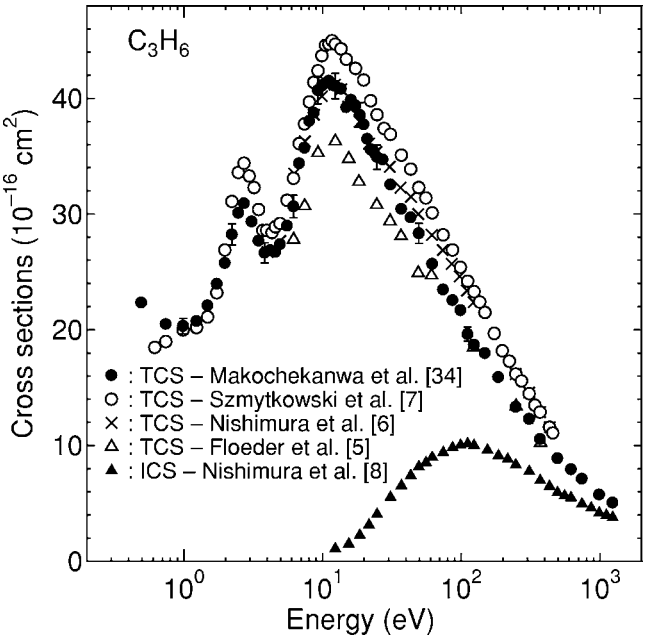

FIG. 4. C_3H_6 electron impact TCSs and ICSs from the literature, including the TCS results from our preliminary report [34].

3. C_3H_6

Figure 4 shows the literature TCS data, together with our preliminary results [34], and the ICSs of Nishimura and Tawara [8]. All four TCS results show similarity in energy dependence over all the energy range of overlap, except for the region below 1 eV. In short, these TCS results are characterized by (i) the rising trend below 1 eV for our result versus a decreasing one for the result of Szmytkowski *et al.* [7], (ii) a rather narrow resonance peak at about 2.2 eV, (iii) the main resonance peak centered at about 9.5 eV, (iv) a change of slope at ~40 eV, and (v) the rather monotonic decrease toward 1000 eV.

Once again as a method for studying the nature and origin of these peaks in the TCSs we carried out electron impact vibrational excitation experiments, since this is a channel usually associated with shape resonances, as discussed above for *c*-C_3H_6. Figure 5 shows the C_3H_6 electron impact energy loss spectrum and the spectra for the bending and stretching vibrational modes.

(i) The rising trend below 1 eV should be associated with the enhanced scattering at these lower energies in C_3H_6 due to the presence of the small electric dipole moment (0.366 D) and the relatively large polarizability (6.26×10^{-30} m^3). (ii) The peak at about 2.2 eV should have contributions from the shape resonance due to vibrational excitation of the molecules, as can be clearly seen in the vibrational excitation functions of the bending vibrational mode v_3 with a peak at around 2 eV for these molecules in Fig. 5. This channel proceeds via formation of the transient $C_3H_6^-$ ion due to the incident electron being trapped temporarily into valence orbitals with C=C antibonding character, i.e., the lowest unoccupied molecular orbital (LUMO), which is a π^* shape resonance according to studies by Winstead *et al.* [10]. In Fig. 5(b) we also include the result we obtained for a similar C

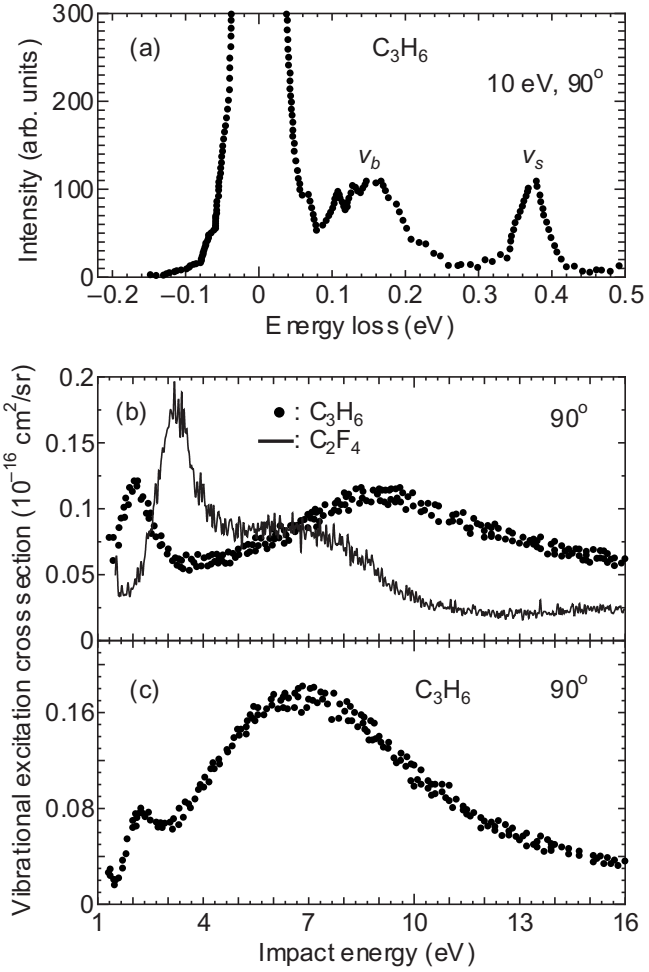

FIG. 5. (a) C_3H_6 electron impact energy loss spectrum measured at 10 eV and scattering angle 90°. (b) Vibrational excitation cross sections for the C_3H_6 bending mode at 90° and energy loss 0.12 eV. C_2F_4 data from Ref. [37] are also shown for 90° and energy loss 0.16 eV for comparison. (c) Vibrational excitation cross sections for the C_3H_6 stretching mode at 90° and energy loss 0.37 eV.

=C double-bond-containing molecule C_2F_4 [37]. The ~1 eV shift in the position of this peak in C_2F_4 compared to C_3H_6 is a characteristic fluorination effect, also observed and discussed in the cases of the TCSs for C_3F_6 vs C_3H_6, C_2F_4 vs C_2H_4 [34], and C_2H_6 vs C_2F_6 [31]. In comparing the results in Figs. 5(b) and 5(c), it is also observed that the cross section for this 2.2 eV peak in C_3H_6, albeit now a stretching mode in Fig. 5(b), decreases with increase in the loss energy. This is contrary to the increase observed for the 8.5 eV peak, which not only moves by about 2 eV to lower energies but also increases in magnitude of the cross section. (iii) The main resonance peak at about 9.5 eV in the TCSs should be attributable to the A_1 symmetry type of the shape resonance that we have observed to be characteristic of hydrocarbons, resulting in peaks in this region, although contributions from other several inelastic scattering processes, e.g., the vibrational excitation shown in Fig. 5, should also be significant [36].

4. Comparison of our TCSs with other results

For the reason pointed out for c-C_3H_6 above, we carry out a brief comparison of our preliminary results with those by other groups from the literature. These results are shown in Fig. 4. Except for the region below 1 eV where the current data rise versus a decreasing trend for the Szmytkowski *et al.* [7] results, our TCSs agree well in structure with the other three measurements. However, some magnitude differences are observed at the peaks. For example, our result is smaller than the largest of the three (Szmytkowski *et al.*) by more than 12% at 2.2 and 9.5 eV, while greater than the lowest of the three (Floeder *et al.*) by about 15% at 9.5 eV. The origin of these differences is not clear, especially with the Szmytkowski *et al.* result above 8 eV.

B. Positron impact

The positron TCS results presented here are not corrected for possible effects of the forward scattering discussed in Sec. II A above. Therefore it is possible that our cross sections are underestimated by a few percent, although the energy dependence is correct.

1. c-C_3H_6

In Fig. 6(a) we show the current c-C_3H_6 positron TCSs, in comparison with the only available data of Floeder *et al.* [5]. These TCS results show some peculiar peak structures not usually expected in positron TCSs. These include the peak structure centered at about 1.8 eV, before the typical hydrocarbon main peak at about 9.5 eV. However, this main peak is split into two by the dip at about 13 eV, to give peaks at about 7 and 25 eV. Thereafter, the TCSs rather smoothly decrease toward 600 eV. The 1.8 eV peak lies below the threshold for positronium formation, E_{Ps}=3.06 eV, which makes it difficult to discuss its nature and origin based on known physics. However, this could be a signature of the recently reported positron-molecule bound state condition, i.e., a case whereby an incoming positron gets temporarily trapped by the polarized electron cloud of the target molecule [4]. The 7 eV peak structure could be partly made up of the contribution from the positronium formation channel as well. It is not clear what the cause of the dip observed at about 13 eV could be. However, it is possible that the dip could be due to the combined effect of the rising positronium formation and the ionization cross sections, i.e., with thresholds E_{Ps}=3.06 eV and E_{ion}=9.86 eV, respectively, and peaking at different energies.

In the comparative study of the current positron TCS with those of Floeder *et al.*, good qualitative and quantitative agreement is obtained over the whole range above 7 eV. However, their data exceed ours in magnitude below 7 eV and do not show a pronounced dip at about 13 eV, as our data clearly do.

2. C_3H_6

The current C_3H_6 positron TCS results are shown in Fig. 6(b) in comparison with the only available data, those of Floeder *et al.* [5]. These TCSs are characterized by (i) the seemingly rising trend indicated by the lowest point at 0.2 eV, (ii) the small peak-like feature at 0.8 eV, (ii) the rather gradually rising trend above 1.6 eV, (iii) the broad main peak spanning the range 3–30 eV, split into two by a minimum at about 10 eV, (iv) a change of slope at about 80 eV, and (vi) a monotonically decreasing trend up to 1000 eV.

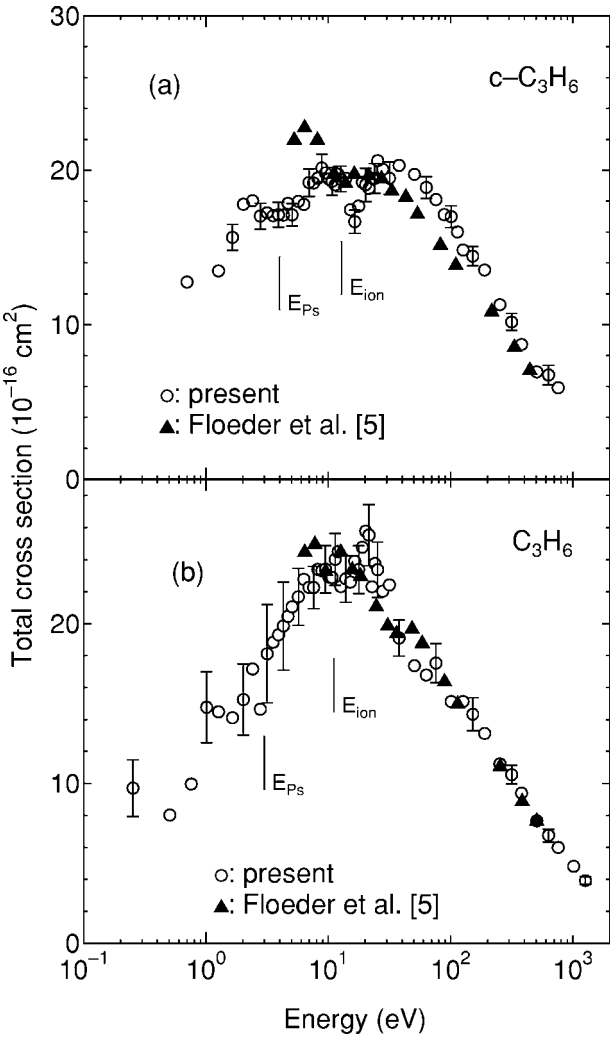

FIG. 6. Present positron TCSs for (a) c-C_3H_6 and (b) C_3H_6, in comparison with those of Floeder *et al.* [5]. The vertical bars show the positions of the thresholds for positronium formation, E_{Ps}, and ionization, E_{ion}.

(i) It is surely not suitable to make any argument based on the rise seemingly indicated by the 0.2 eV single point, given the error rate involved in our data at this lowest energy. However, it is an interesting observation as, if real, it indicates the long-range dipole interaction showing up in this form of increasing TCS at low energies, even in positron scattering. We take interest in this because so far, although we have carried out a number of systematic studies hunting for this dipole effect; we have succeeded in observing it in electron impact TCSs but not in positron TCSs. See, for example, our studies on the strongly polar molecules CH_3Cl (1.892 D), CH_3Br (1.882 D), and CH_3I (1.620 D) [38], i.e., molecules with permanent dipole moments more than six times that for C_3H_6 (0.366 D). We could not observe this

effect in positron TCSs in the limit of our lowest energy of measurement of 0.2 eV. (ii) The peak-like structure observed at 0.8 eV is very rare in positron scattering and we are not sure what its exact origin is. In electron scattering, at such a low energy, such a feature would most probably be due to either vibrational excitation or some bound state of the incoming electron with the molecule, giving a shape resonance. Further study is awaited for its elucidation. (iii) The rather smooth rising trend above 1.6 eV toward the main peak is also a deviation from our systematic observation that, for pure hydrocarbons, the opening up of the positronium formation channel, with threshold E_{Ps}=2.93 eV for C_3H_6, is followed by a sudden rise in the TCS [39]. (iv) It is not clear what the cause of the dip observed at about 10 eV could be. However, it is possible that the physics to be learnt from this phenomenon does not lie in the dip itself but possibly in the rising ionization cross section, to produce the higher-energy side peak at about 16 eV, against the background of a decreasing trend in the TCSs.

In the comparative study of the current positron TCSs with those of Floeder *et al.*, good qualitative and quantitative agreement is obtained over the whole range of overlap above 60 eV. However, although their data also show a higher-energy shoulder, the location is about 40 eV compared to ours at about 50 eV. Again, their TCSs miss the second peak at about 16 eV, i.e., their data show only one peak compared to the split-peak phenomenon in our result.

C. Comparison between electron and positron impact TCSs

1. c-C_3H_6

Figures 7(a) and 7(b) show the current electron and positron TCSs and the 5–400 eV data of Floeder *et al.*, respectively. The main features in the comparative study between these electron and positron TCSs can be summarized as follows. (i) Whereas the positron TCSs continue to decrease below 1.5 eV, the electron TCSs seem to start rising. Such a rising trend may be associated with the polarizability (5.66×10^{-30} m^3) in these molecules at these low energies leading to slight enhancement of scattering events due to long-range scattering. However, why such scattering would be observable only in electron scattering and not in positron TCSs remains an open question. (ii) The positron TCSs nearly equal the electron TCSs at 1.5–3 eV. (iii) Electron TCSs are greater than positron TCSs at energies 5–100 eV; the largest difference being at the main peak at about 10 eV, where it reaches 60%. It is worth noting that the Floeder *et al.* results also show a similar pattern over the whole energy range of their measurements. The intermediate energy range differences between electron and positron TCS magnitudes owe their origin to the larger contribution of resonances in electron scattering compared to positron scattering. (iii) Our results show that above about 200 eV electron and positron TCSs tend toward merging with each other. However, this is only implied in the Floeder *et al.* results as they do not clearly observe this phenomenon. Nevertheless, this observation is rather to be expected from the Born approximation.

2. C_3H_6

Figures 8(a) and 8(b) show the current electron and positron TCSs and the 5–400 eV data of Floeder *et al.*, respectively. Observations from the results shown in this figure are summarized as follows. (i) In the limit of experimental errors involved in the positron result at the lowest value of 0.2 eV, both TCSs seem to show a rising trend with decreasing energy toward 0 eV and a low-energy peak structure, at 0.8 eV for positron and 2.2 eV for electron impact. They both rise to show maxima at about the same energy range, albeit broader and split into two for positron TCSs. (ii) Electron TCSs are greater than positron TCSs at all energies below 200 eV; the largest difference being at the main peak at about 10 eV, where it reaches 75%. Although the Floeder *et al.* results [Fig. 8(b)] show a similar pattern below 200 eV, i.e., the difference is greatest at the peak energy of about 10 eV as well, somehow the magnitudes of their data seem to come close to each other at their lowest energy of 5 eV. Nevertheless, as pointed out already above, these huge differences at intermediate impact energies between electron and positron TCS magnitudes owe their origin to the larger contribution of resonances in electron scattering compared to positron scattering. (iii) Beyond 200 eV, however, these electron and

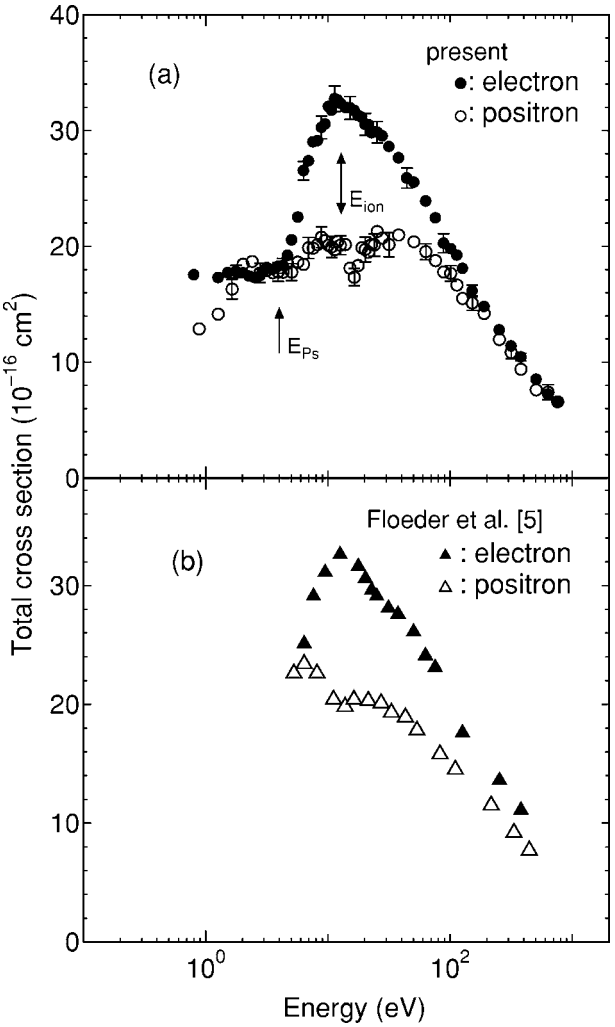

FIG. 7. c-C_3H_6: (a) present and (b) Floeder *et al.* [5] electron and positron TCSs. The arrows show the positions of the thresholds for positronium formation, E_{Ps}, and ionization, E_{ion}. Error bars show total uncertainties derived as explained in the text.

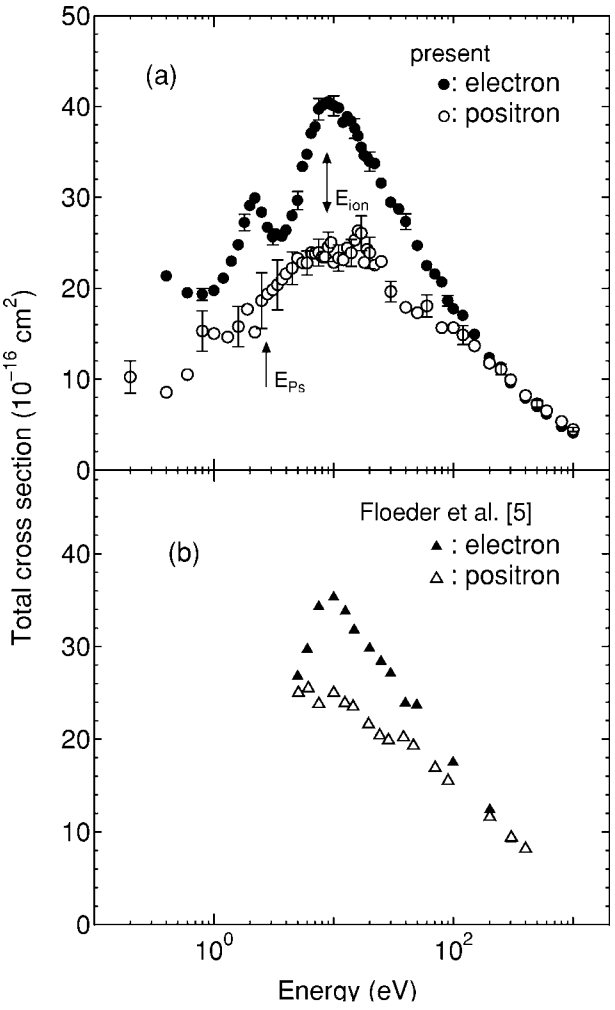

FIG. 8. C_3H_6 (a) present and (b) Floeder *et al.* [5] electron and positron TCSs. See caption of Fig. 7 for other details.

positron TCSs tend toward merging with each other, a rather expected observation since at these energies only the long-range interaction dominates the scattering event, and as a result just the first Born term is sufficient for accurate description of scattering.

IV. CONCLUSION

In this paper, we report experimental measurements of electron and positron impact total and vibrational excitation cross sections for c-C_3H_6 and C_3H_6. For both molecules, electron impact vibrational excitation cross sections for the two strongest modes, bending and stretching, have been employed in probing resonances in electron TCSs. c-C_3H_6: weak peaks have been observed in electron TCSs at about 1.5 and 2.6 eV, a significant shoulder at about 6 eV, the hydrocarbon characteristic peak at about 9.5 eV, and the change of slope at 40 eV. Vibrationally inelastic excitation has been associated with these structures, except the one at 40 eV. Positron TCSs show peaks at 1.8 eV and the main one split into two by a dip at about 13 eV. Positron and electron TCSs nearly equal each other at 1.5–3 eV, the latter become greater than the former in the main peak regions, and the two tend toward merging above 200 eV, as expected from the first Born approximation. For C_3H_6, in electron impact TCSs, the rising trend below 1 eV has been attributed to the dipole-moment-induced long-range scattering effect, while the 2.2 eV peak has been attributed to a π^* shape resonance characteristic of a double-bond-containing molecule. The careful study of vibrational excitation cross sections also shows that the 2.2 eV peak has significant contributions from the vibrational excitation channel. The 9.5 eV peak was attributed to the A_1 symmetry type of shape resonance that we have observed to be characteristic of all hydrocarbons. Positron TCSs show an unexpected richness in structure, an indication of the beginning of a rise of the TCS at 0.2 eV, a peak feature at 0.8 eV, and a broad 3–30 eV main peak split into two at about 10 eV. The combined effects of resonances in electron TCSs result in greater TCSs for the former than the latter below 200 eV, with the two showing a tendency toward merging above this energy, as expected from the first Born approximation.

ACKNOWLEDGMENTS

The work was supported in part by a Grant-in-Aid from the Ministry of Education, Science, Technology, Sport and Culture, Japan, the Japan Society for the Promotion of Science (JSPS), the Japan Atomic Energy Research Institute (JAERI), and a Cooperative Research Grant from the National Institute for Fusion Science (NIFS).

[1] N. Duric, J. Cadéz, and M. Kurepa, Int. J. Mass Spectrom. Ion Process. **108**, R1 (1991).
[2] T. Makabe, Adv. At., Mol., Opt. Phys. **44**, 127 (2001).
[3] H. Tawara, Y. Itikawa, H. Nishimura, H. Tanaka, and Y. Nakamura National Institute for Fusion Science (Nagoya) Report No. NIFS-DATQA-6, 1990 (unpublished).
[4] C. M. Surko, G. F. Gribakin, and S. J. Buckman, J. Phys. B **38**, R57 (2005).
[5] K. Floeder, D. Fromme, W. Raith, A. Schwab, and G. Sinapius, J. Phys. B **18**, 3347 (1985).
[6] H. Nishimura and H. Tawara, J. Phys. B **24**, L363 (1991).
[7] C. Szmytkowski and S. Kwitnewski, J. Phys. B **35**, 2613 (2002).
[8] H. Nishimura and H. Tawara, J. Phys. B **27**, 2063 (1994).
[9] H. Deutsch, K. Becker, J. K. Janev, M. Probst, and T. D. Mark, J. Phys. B **33**, L865 (2000).
[10] C. Winstead, Q. Sun, and V. McKoy, J. Chem. Phys. **96**, 4246 (1992).

[11] T. Beyer, B. M. Nestmann, B. K. Sarpal, and S. D. Peyerimhoff, J. Phys. B **30**, 3431 (1997).
[12] R. Curik and F. Gianturco, J. Phys. B **35**, 717 (2002).
[13] C. Makochekanwa, H. Kato, M. Hoshino, H. Tanaka, H. Kubo, M. H. F. Bettega, A. R. Lopes, M. A. P. Lima, and L. G. Ferreira, J. Chem. Phys. **124**, 024323 (2006).
[14] M. Allan, in *Electron Collisions with Molecules, Clusters and Surfaces*, edited by H Ehrhardt and L A Morgan (Plenum Press, New York, 1994), p. 105.
[15] Y. Jiang, J. Sun, and L. Wan, J. Phys. B **30**, 5025 (1997).
[16] M. Allan, J. Am. Chem. Soc. **115**, 6418 (1993); J. Chem. Phys. **105**, 3559 (1996).
[17] R. Curik and F. Gianturco, J. Phys. B **35**, 1235 (2002).
[18] K. H. Sze and C. E. Brion, J. Electron Spectrosc. Relat. Phenom. **57**, 117 (1991).
[19] H. H. Brongersma and L. J. Oosterhoff, Chem. Phys. Lett. **3**, 437 (1969).
[20] M. P. Banjavcic, T. A. Daniels, and K. T. Leung, Chem. Phys. **155**, 309 (1991).
[21] H. Koizumi, T. Yoshimi, K. Shinsaka, M. Ukai, M. Morita, Y. Hatano, A. Yagishita, and K. Ito, J. Chem. Phys. **82**, 4856 (1985).
[22] H. Basch, M. B. Robin, N. A. Kuebler, C. Baker, and D. W. Turner, J. Chem. Phys. **51**, 52 (1969).
[23] C. R. Bowman and W. D. Miller, J. Chem. Phys. **42**, 681 (1965).
[24] C. W. Duncan and I. C. Walker, J. Chem. Soc., Faraday Trans. 2 **70**, 577 (1974).
[25] K. E. Johnson, D. B. Johnston, and S. Lipsky, J. Chem. Phys. **70**, 3844 (1979).
[26] O. Sueoka, S. Mori, and A. Hamada, J. Phys. B **27**, 1452 (1994).
[27] M. Kimura, C. Makochekanwa, and O. Sueoka, J. Phys. B **37**, 1461 (2004).
[28] K. R. Hoffman, M. S. Dababneh, Y. F. Hsieh, W. E. Kauppila, V. Pol, J. H. Smart, and T. S. Stein, Phys. Rev. A **25**, 1393 (1982).
[29] O. Sueoka and S. Mori, J. Phys. B **19**, 4035 (1986).
[30] A. Hamada and O. Sueoka, J. Phys. B **27**, 5055 (1994).
[31] O. Sueoka, C. Makochekanwa, and H. Kawate, Nucl. Instrum. Methods Phys. Res. B **192**, 206 (2002).
[32] H. Tanaka, T. Ishikawa, T. Masai, T. Sagara, L. Boesten, M. Takekawa, Y. Itikawa, and M. Kimura, Phys. Rev. A **57**, 1798 (1998).
[33] S. K. Srivastava, A. Chutjian, and S. Trajmar, J. Chem. Phys. **63**, 2659 (1975).
[34] C. Makochekanwa, H. Kato, M. Hoshino, H. Cho, M. Kimura, O. Sueoka, and H. Tanaka, Eur. Phys. J. D **35**, 249 (2005).
[35] B. M. Nestmann, J. Phys. B **31**, 3929 (1998).
[36] H. Tanaka and L. Boesten, in *Proceedings of the XIX International Conference on The Physics of Electronic and Atomic Collisions, Whistler, Canada*, edited by L. J. Dube *et al.* (AIP, Woodbury, NY, 1995), p. 279.
[37] R. Panajotovic, M. Jelisavcic, R. Kajita, T. Tanaka, M. Kitajima, H. Cho, H. Tanaka, and S. J. Buckman, J. Chem. Phys. **121**, 4559 (2004).
[38] M. Kimura, O. Sueoka, C. Makochekanwa, H. Kawate and M. Kawada, J. Chem. Phys. **115**, 7442 (2001).
[39] C. Makochekanwa, O. Sueoka, and M. Kimura, Nucl. Instrum. Methods Phys. Res. B **247**, 79 (2006).